

REPORT DOCUMENTATION PAGE

AFRL-SR-AR-TR-02-

0233

Public reporting burden for this collection of information is estimated to average 1 hour per response, including the time for reviewing the data needed, and completing and reviewing the collection of information. Send comments regarding this burden estimate or any other aspect of this collection of information, including suggestions for reducing this burden, to Washington Headquarters Services, Directorate for Information Operations and Reports, 1215 Jefferson Davis Highway, Suite 1204, Arlington, VA 22202-4302, and to the Office of Management and Budget, Paperwork Reduction Project (0704-0188), Washington, DC 20503.

1. AGENCY USE ONLY (Leave blank)		2. REPORT DATE		3. REPORT TYPE AND DATES COVERED 15 Jun 97 to 14 Jun 01 FINAL	
4. TITLE AND SUBTITLE 97-AASERT Augmented Student participation in Theoretical Investigation of point defects and defect complexes in LT GaAs				5. FUNDING NUMBERS 61103D 3484/TS	
6. AUTHOR(S) Prof. Morgan					
7. PERFORMING ORGANIZATION NAME(S) AND ADDRESS(ES) Wayne State Univ 656 West Kirby Room 4002 FAB Detroit MI 48202				8. PERFORMING ORGANIZATION REPORT NUMBER	
9. SPONSORING/MONITORING AGENCY NAME(S) AND ADDRESS(ES) AFOSR/NE 801 North Randolph Street Rm 732 Arlington, VA 22203-1977				10. SPONSORING/MONITORING AGENCY REPORT NUMBER F49620-97-1-0479	
11. SUPPLEMENTARY NOTES					
12a. DISTRIBUTION AVAILABILITY STATEMENT APPROVAL FOR PUBLIC RELEASE; DISTRIBUTION UNLIMITED				12b. DISTRIBUTION CODE	
13. ABSTRACT (Maximum 200 words) This AASERT grant is a supplementary grant which has provided funding for additional student involvement in the work supported by AFOSR grant Number 49620-96-1-0162, "Theoretical Investigation of Point Defects and Defect Complexes in Low-Temperature-Grown GaAs". The major aim of this research has been a theoretical investigation of (1) important point defects and defect complexes in low-temperature-grown (LT) GaAs and (2) the microscopic processes occurring at the surface during growth of GaAs films, which determine how much excess arsenic will be incorporated into the material.					
14. SUBJECT TERMS				15. NUMBER OF PAGES	
				16. PRICE CODE	
17. SECURITY CLASSIFICATION OF REPORT UNCLASSIFIED		18. SECURITY CLASSIFICATION OF THIS PAGE UNCLASSIFIED		19. SECURITY CLASSIFICATION OF ABSTRACT UNCLASSIFIED	
				20. LIMITATION OF ABSTRACT UL	

20020816 067

Final Technical Report

Augmented Student Participation in Theoretical Investigation of Point Defects and Defect Complexes in Low-Temperature-Grown GaAs

GRANT NUMBER:

F49620-96-1-0479

PRINCIPAL INVESTIGATOR:

Caroline G. Morgan

Department of Physics and Astronomy

Wayne State University

Detroit, MI 48202

PERIOD OF SUPPORT:

June 15, 1997-June 14, 2001

Table of Contents

1. Introduction	3
2. Properties of Point Defects and Defect Complexes in Arsenic-rich GaAs	5
2.1 Arsenic Interstitials: Can they be important, and if so, when?	5
2.1(a) Convergence, relaxation, defect states, and formation energy of arsenic interstitials	10
2.1(b) Relative formation energies and equilibrium concentrations of native point defects containing excess arsenic in the As-rich limit	21
2.1(c) Charge transition levels in the experimental gap	24
2.1(d) Arsenic interstitial diffusion	26
2.2 Arsenic Interstitial Pairs: Beginnings of an Interstitial Cluster	29
2.3 Bond-order Potentials and Radiation Damage	33
3. Growth Processes and Incorporation of Excess Arsenic at Growth	34
3.1 Decorated and Undecorated Kinks: Structures, Formation Energies, and Contribution to Surface Stoichiometry	34
4. References	40
5. Students Supported under this Grant	43
6. Publications/Presentations/Degrees Granted	44

1. Introduction

This AASERT grant is a supplementary grant which has provided funding for additional student involvement in the work supported by AFOSR grant Number 49620-96-1-0162, "Theoretical Investigation of Point Defects and Defect Complexes in Low-Temperature-Grown GaAs". The major aim of this research has been a theoretical investigation of

- (1) important point defects and defect complexes in low-temperature-grown (LT) GaAs and
- (2) the microscopic processes occurring at the surface during growth of GaAs films, which determine how much excess arsenic will be incorporated into the material.

In collaboration with researchers supported by the parent grant, the students supported by this grant have used first-principles pseudopotential calculations to identify and study the low energy defect configurations which can accommodate the excess arsenic that is present in LT GaAs, and to study the technologically important dopant beryllium. They have studied the interactions between these defects, and the mechanisms and energetics of defect motion and transformation (including diffusion, transitions into and out of metastable states, and complex formation and breakup). They have studied the structure of defects at the GaAs surface, and generated simulated STM images of defects containing excess arsenic at the growth surface and at the cleavage surface for comparison with experiment, using the Tersoff-Hamann method.¹

In order to accomplish this work, the students supported by this grant performed density-functional calculations using both the local density approximation (LDA) and the generalized gradient approximation (GGA),² to maximize accuracy and facilitate comparison with earlier calculations. With the exception of a couple of early papers cited in section 2, which used calculations based on the Sankey-Niklewski method,³ which is implemented in terms of a basis of pseudoatomic orbitals, all of the work reported here was based on fully self-consistent calculations using a plane wave basis and the codes developed at the Fritz-Haber-Institut der Max-Planck-Gesellschaft.⁴ These calculations used fully separable, norm-conserving pseudopotentials⁵⁻⁷ constructed from an all-electron atomic calculation to describe the electron-ion interaction. Gonze's analysis⁸ was used to confirm that unphysical ghost states were not present in the separable representation.

The work which is discussed in detail here, especially the work on arsenic interstitials, interstitial diffusion, and interstitial-containing complexes, has been carried out primarily by students supported by this grant. Detailed results of convergence studies for arsenic interstitials carried out by the students are reported in some detail in section 2.1(a), while other results which are (or will soon be) available and presented in detail in the published papers and Ph.D. theses are summarized in a shorter form.

Other work which was carried out primarily by researchers supported by the parent grant with smaller contributions from students supported by this grant is described in the final report for the parent grant, F49620-96-1-0162. In particular, the work on substitutional beryllium and its interactions with arsenic antisites and on arsenic-interstitial-arsenic-antisite complexes, which was described in the final report for the parent grant, F49620-96-1-0162, was carried out in a close collaboration between researchers supported by this grant and by the parent grant.

2. Properties of Point Defects and Defect Complexes **in Arsenic-rich GaAs**

2.1 Arsenic Interstitials: Can they be important, and if so, when?

Interstitials are the most structurally complex and least well understood of the elementary point defects in semiconductors. They are difficult to observe directly in experiments. For example, even though arsenic interstitials must be created by irradiation of GaAs with sufficiently energetic particles, and they can subsequently be observed to recombine with arsenic vacancies when the sample is heated above 220 °C, isolated arsenic interstitials have not been observed directly in EPR, electrical, or optical experiments.⁹

It has been argued based on a thorough analysis¹⁰⁻¹² of a variety of experimental data including titration experiments¹³ and measurements of density and lattice parameter¹⁴ that melt-grown GaAs is always As-rich unless the concentration of Ga in the melt is substantially greater than 50 %, and that this deviation from stoichiometry is due primarily to the creation of large numbers of As interstitials (As_i) during growth.

In particular, Hurle has argued¹⁰ that the measured deviation of the mass per unit cell as a function of arsenic concentration in the melt must be explained by arsenic interstitials and/or arsenic vacancies, since the number of arsenic antisites which would be required to fit the data is unrealistically large (up to several percent), due to the small difference between the atomic masses of arsenic and gallium. Hurle's work also contains an extensive thermodynamic analysis, including estimates of the mass action constants for the formation of all the neutral native point defects. These estimates are derived by fitting to a large quantity of experimental data on both doped and undoped GaAs, under the assumption that native defect and dopant concentrations are near equilibrium close to the melting point and during high temperature growth from the melt or from solution.

In the high temperature growth regime, observations of defects tentatively described as high concentrations or diffuse "clouds" of arsenic interstitials have been reported in GaAs grown by the horizontal Bridgman and liquid-encapsulated Czochralski methods, based on X-ray diffuse

scattering¹⁵⁻¹⁷ and quasi-forbidden X-ray reflection intensity measurements¹⁸. However, the atomic composition and microscopic structure of these defects cannot be unambiguously determined from these experiments.

Gallium arsenide grown by arsenic-rich molecular beam epitaxy at low temperature (LT GaAs) is a semi-insulating material with a host of potentially useful applications.¹⁹ This material contains up to 1.5 % excess As,²⁰ which is accommodated by high concentrations of point defects in unannealed samples, and arsenic precipitates plus somewhat lower concentrations of point defects in annealed samples. Concentrations of As antisites (As_{Ga}) up to 10^{20} cm^{-3} are observed in LT GaAs, as measured by electron paramagnetic resonance (EPR),²¹ near-infrared absorption (NIRA) and magnetic circular dichroism of absorption (MCDA),²² and scanning tunneling microscopy (STM).²³ Concentrations of Ga vacancies (V_{Ga}) up to 10^{18} cm^{-3} are measured in LT GaAs by slow positron annihilation.²⁴ Ion channeling experiments have been interpreted as providing evidence for large concentrations of As interstitials in LT GaAs.²⁰ However, it was later pointed out that the observed high concentration of atoms in the channel near the normal arsenic lattice sites could also be due to outward relaxation of the nearest neighbors of the As antisites.^{22,25}

Within certain well defined limits of the growth parameters for LT GaAs, a linear correlation between the neutral As_{Ga} concentration and the lattice dilation has been found.^{22,24} It was therefore proposed that As_{Ga} are the dominant defects which determine the lattice expansion for growth within this regime. Staab *et al.*²⁵ used a self-consistent density-functional-based tight-binding method to study the lattice distortion induced by point defects in As-rich GaAs, and concluded that only As_{Ga} are necessary to understand the observed lattice expansion in the regime where the linear correlation is observed, and that if concentrations of isolated As_i comparable to the measured concentrations of As_{Ga} were also present, the lattice expansion would be three times greater than is experimentally observed. However, Luysberg *et al.* have reported that when the As/Ga flux ratio is increased beyond a beam equivalent pressure (BEP) ratio of 20, there is a departure from the linear correlation between lattice dilation and antisite concentration.²⁴ It was pointed out that other defects must be present to account for the deviation from stoichiometry and the lattice expansion at high As/Ga flux ratios.²⁴

Nonequilibrium processes such as diffusion and compositional intermixing at interfaces can also be strongly affected by point defects that are present in high concentrations. Since the point defects which have been unambiguously documented as present in high concentrations in LT GaAs, As_{Ga} and V_{Ga} , occupy sites on the gallium sublattice, they cannot contribute directly to interdiffusion on the arsenic sublattice. However, substantial concentrations of arsenic interstitials may affect interdiffusion on the arsenic sublattice. For example, an experimental study showing a positive dependence of GaAsP/GaAs and GaAsSb/GaAs interdiffusion on arsenic pressure has indicated that a kickout mechanism involving arsenic interstitials is the dominant process for the As-P and As-Sb interdiffusion in the material studied.²⁶

Similarly, annealing LT-GaAs delta-doped with Sb was found to produce substantially greater compositional intermixing than annealing conventional stoichiometric GaAs similarly delta-doped.²⁷ This enhancement of As-Sb interdiffusion was attributed to an oversaturation of arsenic interstitials in the LT GaAs samples, resulting from the balance of arsenic interstitials with arsenic clusters and all the other excess-arsenic-containing defects in the material. The effective activation energy for As-Sb interdiffusion in LT GaAs deduced from this work, 0.6 ± 0.15 eV,²⁷ is reasonably close to the migration energy of 0.5 eV for arsenic interstitials deduced from annealing experiments on defects produced by electron irradiation,⁹ as well as to migration energies subsequently ascribed to arsenic interstitial defects produced in GaAs by other means. The concentration of arsenic interstitials required to produce sufficient oversaturation to eliminate completely any contribution of the interstitial formation energy to the activation energy for As-Sb intermixing measured in the LT GaAs sample was estimated to be roughly 10^{18} cm^{-3} , using Hurle's thermodynamic analysis in conjunction with the experimental data.²⁷

Theoretical attempts to obtain a picture of the microscopic structure and properties of the lowest energy arsenic interstitial configuration(s) began with the work of Baraff and Schlüter, who used density functional Green's function calculations to investigate the energies of reactions creating native defects with T_d symmetry in GaAs, including arsenic interstitials in the two tetrahedral sites.²⁸ The effects of lattice relaxation were ignored. Baraff and Schlüter concluded that simple tetrahedral arsenic interstitials were less likely to occur than vacancy and antisite

defects under all equilibrium conditions, although they could not rule out the possibility that other, more complicated interstitial configurations might have a lower energy.²⁸

Jansen and Sankey calculated the formation energies for unrelaxed native defects with tetrahedral symmetry in GaAs, including arsenic interstitials in tetrahedral sites, using a density-functional pseudopotential method with a basis set of pseudo-atomic orbitals and a single special *k*-point in supercells containing about 32 atoms.²⁹ In order to calculate the formation energies for individual defects instead of reaction energies for defect reactions which conserve the number of atoms of each species, they were required to choose a value for the arsenic chemical potential (or equivalently, for the gallium chemical potential). An arbitrary value was chosen, corresponding to the condition that the formation energies for neutral gallium vacancies and for neutral arsenic vacancies should be equal. Jansen and Sankey concluded that arsenic interstitials in tetrahedral sites should be less numerous than vacancies and antisites in GaAs under equilibrium conditions,²⁹ in agreement with Baraff and Schlüter.

Zhang and Northrup used density functional theory (DFT) within the local density approximation (LDA) and supercells of about 32 atoms to calculate the formation energies for vacancies, antisites, and tetrahedral interstitials in GaAs as a function of arsenic chemical potential, over the physically allowable range of chemical potentials, from Ga-rich to As-rich.³⁰ This physically allowable range is set by the heat of formation of bulk GaAs and by the requirement that the arsenic chemical potential may not exceed the chemical potential of bulk arsenic, since the material is in equilibrium with arsenic precipitates in the arsenic-rich limit. The atomic coordinates were allowed to relax in these calculations, within the constraints imposed by the tetrahedral symmetry. In agreement with the previous work, Zhang and Northrup found that antisites and/or vacancies should be more numerous than arsenic interstitials in tetrahedral sites under all equilibrium conditions.³⁰

Chadi used DFT-LDA calculations and 33-atom supercells to investigate many different types of bonding configurations for self-interstitials in GaAs, including various split interstitials, as well as hexagonal, two-fold coordinated, and tetrahedral interstitials, all fully relaxed within the constraints of the chosen symmetry.³¹ He found that the lowest energy configuration for arsenic interstitials in the neutral or -1 charge state is a split interstitial consisting of two As

atoms sharing an arsenic lattice site, displaced from this site in opposite directions along a $\langle 110 \rangle$ -like axis, while the lowest energy configuration for positively charged arsenic interstitials in the +1 or +2 charge state is a split interstitial consisting of an As atom and a Ga atom sharing a gallium lattice site, displaced from this site in opposite directions along a $\langle 100 \rangle$ -like axis. Since we will be interested below primarily in arsenic interstitials in semi-insulating or n-type GaAs, we will use the notation $\text{As}_i\text{-As}$ for the lowest energy arsenic split interstitial with two atoms sharing an arsenic site, which should be the lowest energy interstitial configuration in semi-insulating or n-type material, and we will use the notation $\text{As}_i\text{-Ga}$ for the arsenic split interstitial with two atoms sharing a gallium site, which should be the lowest energy configuration in p-type material.

Chadi's work also showed that neutral arsenic interstitials, which have unpaired spins, are unstable relative to formation of a pair of +1 and -1 charged interstitials - *i.e.* arsenic interstitials form a negative-U system. This suggested that arsenic interstitials may not be observable in EPR experiments.³¹ Chadi reported the relative energies for the most energetically favorable arsenic interstitial configurations in each of these charge states, including in each case a number of metastable configurations somewhat higher in energy than the lowest energy configurations, all of which were more complicated than the simple tetrahedral configurations.³¹ However, since Chadi did not report absolute interstitial formation energies as a function of arsenic chemical potential, no comparison with the formation energies of defects involving a different number of excess arsenic atoms, such as arsenic antisites, was possible from this work.

Joseph Landman, the first student to use resources supported by this grant to complete his Ph.D., investigated³² the relative formation energies of the point defects containing excess As, As_{Ga} , V_{Ga} , and the lowest energy As_i configuration in semi-insulating or n-type, As-rich GaAs, $\text{As}_i\text{-As}$, using DFT-LDA-based calculations with the Harris-Foulkes functional and a basis of pseudo-atomic orbitals.^{3,33} He placed the defects in 64-atom supercells, and estimated summations in \mathbf{k} -space by using a single Chadi and Cohen special point.³⁴ Since Harris-Foulkes, pseudoatomic-orbital calculations do not give as accurate results for semiconductor heats of formation or for the relative energies of compound semiconductor and pure, metallic phases as fully self-consistent DFT-LDA calculations with a sufficiently large basis of plane waves, he did

not use this method to calculate the arsenic chemical potential in the arsenic-rich limit. Instead, the relative formation energies of the tetrahedral As_i with arsenic nearest neighbors, As_{Ga} , and V_{Ga} in the arsenic-rich limit for the chemical potential were taken from information given by Zhang and Northrup,³⁰ and the relative formation energy of As_i -As was determined by Landman *et al.*'s result³² that the neutral As_i -As is 4 eV lower in energy than the unrelaxed, neutral tetrahedral As_i with arsenic nearest neighbors. Since the tetrahedral interstitial was found to be unstable, relaxing to another configuration in Landman *et al.*'s calculation, he was obliged to compare his results for the ideal, unrelaxed tetrahedral interstitial to Zhang and Northrup's results for a tetrahedral interstitial which had been relaxed while constrained to keep its tetrahedral symmetry. This led to an additional uncertainty in the relative formation energies of zero to 0.8 eV.³² However, Landman *et al.* concluded that As_i -As may have a concentration approaching that of As_{Ga} for certain Fermi levels.³²

2.1(a) Convergence, relaxation, defect states, and formation energy of arsenic interstitials

Since the theoretical investigations described above have been carried out over a long period of time, it has gradually become possible not only to include lattice relaxation and to investigate more complicated interstitial configurations, but also to do more accurate calculations, using larger unit cells and better sets of \mathbf{k} -points for the summations over \mathbf{k} -space. Pöykko *et al.* showed how sensitive calculated defect properties can be to the \mathbf{k} -space sampling method and supercell size in their investigation of the $V_{\text{As}}\text{-Si}_{\text{Ga}}$ complex in GaAs.³⁵ They found that the use of the Γ point can produce misleading results even when supercells are 64 atoms in size, reinforcing the conclusions of Makov *et al.* that the Γ point produces particularly slowly converging results with respect to cell size.³⁶ So it is essential to use a special point mesh in this type of calculation. Furthermore, Puska *et al.* concluded that cell sizes of 128 to 216 atoms are needed to properly assess the physical properties of the silicon vacancy in bulk silicon, because of the dispersion of energy levels and long range ionic relationships.³⁷

Panagiotis Papoulias, the second student to use resources provided by this grant to complete the work for his Ph.D., has investigated the combined effects of cell size and \mathbf{k} -space

sampling on the formation energy, charge state transitions, atomic relaxations, and characterization of localized defect states for arsenic self-interstitials in GaAs.³⁸⁻³⁹ Because of the more ionic nature of the material and the complicated split interstitial defect structure, comparison of his results for interstitials in GaAs to the previous results for vacancies in silicon³⁷ can enhance our understanding of the range of behavior for different defects in different materials. He has also compared the formation energies of the lowest energy split As_i , As_{Ga} , and V_{Ga} at the arsenic-rich end of the range of physically allowed chemical potentials, all calculated by state-of-the-art DFT pseudopotential⁴ calculations with a plane wave basis, using the larger supercells and sets of special k -points which he has determined to be necessary. He and his collaborators (whose work was supported by the parent grant) have used these results to examine the relative concentrations of these defects in equilibrium at growth temperatures, and have used the computed charge transition levels to determine the expected positions of the charge transition levels in the experimental gap.

Mr. Papoulias and his collaborators used the FHMD code⁴ for this investigation, using density-functional theory⁴⁰ within the local density approximation, with the Ceperley-Alder⁴¹ form for the exchange and correlation potentials as parameterized by Perdew and Zunger.⁴² The core electrons were treated in the frozen-core approximation and the ion cores were replaced by fully-separable⁵ norm-conserving pseudopotentials.⁶ Plane waves were included up to an energy cutoff of 10 Ry. The atoms were allowed to relax until the force components were less than 5×10^{-4} hartrees per bohr radius and the zero temperature formation energies changed by less than 5×10^{-6} hartrees per step for at least 100 steps.

To evaluate the defect formation energy, Mr. Papoulias and his collaborators used the formalism of Zhang and Northrup,³⁰ which gives for the formation energy in the As-rich limit at zero temperature

$$\Delta E_f = E(N_{Ga}, N_{As}) - N_{Ga} \mu_{GaAs} - (N_{As} - N_{Ga}) \mu_{As(bulk)} + q \epsilon_F.$$

Here q electrons have been transferred to a reservoir at the Fermi energy ϵ_F in order to produce a defect in the desired charge state. $E(N_{Ga}, N_{As})$ is the zero-temperature total energy produced by the *ab initio* code for a supercell containing the desired defect, the chemical potential μ_{GaAs} is the energy per atomic pair of bulk GaAs, and the arsenic chemical potential in the As-rich limit,

$\mu_{\text{As(bulk)}}$, is the energy per atom of pure bulk As computed using the same *ab initio* code and pseudopotentials. N_{Ga} and N_{As} are the numbers of atoms of each species in the supercell containing the defect. The effects of temperature, which can be important for defect concentrations, will be discussed in Section 2.1(b) below.

Because the zero of the electronic energy levels floats freely,⁴³ different DFT supercell calculations must be aligned in order to obtain the correct charge transition levels. Mr. Papoulias applied the procedure outlined by Kohan *et al.*⁴⁴ in which he first computed the difference between the electrical potential in the supercell with the neutral defect and the electrical potential for the corresponding bulk crystal supercell, averaged over parallel planes, as a function of position along a line normal to the planes. Far from the defect within the supercell, this difference becomes a constant. In order to make the potential far from the neutral defect equal to the corresponding potential in the bulk cell, a uniform shift was applied to the energy levels, yielding the proper alignment of the energy levels of the defect with the energy levels of ideal bulk crystal supercell. The same shift was applied for all charge states of a given defect.

A key shortcoming of the LDA is that it is well-known for underestimating the band gaps of materials. The typical method for dealing with this problem in the bulk is to simply shift the conduction band states up uniformly by the amount needed to reproduce the experimental gap, using the so-called “scissors operator”. More recently, an analytically-based model justifying the rigid shifting upward of all conduction band states by a scissors-type correction has been shown to produce good results for a large number of semiconductors.⁴⁵ Since the LDA can produce similarly large errors in the energies of the deep defect states, it is also important to correct for the errors when determining where the charge transition levels corresponding to deep defect states lie in the experimental gap. Unfortunately, a full GW calculation, which would correct these errors, is not currently possible for the large supercells needed for studies of defects. Therefore, Mr. Papoulias applied the same upward shift to the defect states with predominantly conduction band character as is applied to the conduction band states themselves, while leaving the defect states with predominantly valence band character fixed relative to the valence band edge (VBM).

Mr. Papoulias used cubic supercells with dimensions of either two or three times the computationally determined bulk lattice constant, corresponding to bulk cells of 64 and 216 atoms, along with three different Brillouin zone (BZ) sampling schemes to examine the effects cell size and sampling scheme have on the formation energies and charge transition levels. In order to investigate the most efficient choice of \mathbf{k} points to obtain good results, he did calculations using a 1^3 Monkhorst-Pack (MP) mesh,⁴⁶ a 2^3 MP mesh, and the Γ and L points, which was recommended as a good minimal set of \mathbf{k} points for cubic supercells with no symmetry within the supercell,³⁶ and which was reported to give good structural agreement between calculations and experiments on certain dopants in Si.⁴⁷ Calculations on vacancies in Si comparing different summation schemes show that use of $\Gamma + L$ produces a well converged formation energy in a 64-atom supercell.³⁷

Earlier work on the vacancy in silicon has shown that the neutral vacancy formation energy computed with different \mathbf{k} space sampling schemes converges at different rates with respect to supercell size.³⁷ However, the neutral vacancy formation energy converges faster than the position of the charge transition levels and the defect symmetry for different charge states.³⁷

Mr. Papoulias has added to our understanding of the effects of cell size and sampling scheme by computing formation energies in various charge states for As_i -As in GaAs. Charge was balanced by a uniform background to avoid long-range Coulomb interactions between the supercells. The formation energies obtained by Mr. Papoulias for the excess-arsenic-containing point defects in the arsenic-rich limit, with the GaAs in equilibrium with bulk arsenic, are listed in Table 1, where complete results for the various \mathbf{k} -space sums are included for As_i -As. For comparison, the formation energies of the unrelaxed, ideal tetrahedral As interstitials with As neighbors (As_{i1}) and with Ga neighbors (As_{i2}) are also shown. This table displays formation

Table 1 (included on the following page). Formation energies for excess-arsenic-containing point defects, computed in the As-rich limit. These were calculated with supercells corresponding to the bulk 216 atom cell. The values in the last column are computed with the Fermi level pinned at the (+1/0) transition level of the As antisite defect.

Defect	k-space sum	Charge state	Formation energy (eV) ϵ_F at VBM	Formation energy (eV) semi-insulating ϵ_F
As _{Ga}	MP 2 ³	+2	0.9	2.0
As _{Ga}	MP 2 ³	+1	1.3	1.8
As _{Ga}	MP 2 ³	0	1.8	1.8
As _{Ga}	MP 1 ³	+2	0.9	1.8
As _{Ga}	MP 1 ³	+1	1.1	1.6
As _{Ga}	MP 1 ³	0	1.6	1.6
As _{i1}	MP 2 ³	0	6.9	6.9
As _{i2}	MP 2 ³	0	6.2	6.2
As _i -As	MP 2 ³	+1	3.5	4.1
As _i -As	MP 2 ³	0	3.8	3.8
As _i -As	MP 2 ³	-1	4.4	3.8
As _i -As	MP 1 ³	+1	3.4	3.8
As _i -As	MP 1 ³	0	3.7	3.7
As _i -As	MP 1 ³	-1	4.1	3.7
As _i -As	$\Gamma + L$	+1	3.6	
As _i -As	$\Gamma + L$	0	3.6	
As _i -As	$\Gamma + L$	-1	4.1	
V _{Ga}	MP 2 ³	0	2.9	2.9
V _{Ga}	MP 2 ³	-1	3.0	2.5
V _{Ga}	MP 2 ³	-2	3.1	2.1
V _{Ga}	MP 2 ³	-3	3.4	1.8

energies evaluated for the Fermi level at the VBM, and also for the Fermi level pinned at the position of the (+1/0) charge state transition of As_{Ga} (VBM + 0.54 eV for the 2^3 MP mesh and VBM + 0.45 eV for the 1^3 MP mesh), which was chosen based in the experimental finding that there can be high concentrations of As_{Ga} in As-rich GaAs, and that these high concentrations of As_{Ga} can pin the Fermi energy near this transition level. Using either choice of Fermi level as a reference, the formation energies and the equilibrium concentrations of the defects can be determined as a function of Fermi energy (or doping level). We note that the formation energies of the charged defects depend on the position of the charge transition levels in the gap. The uncertainty in the placement of these charge transition levels that is inherent in LDA calculations, as discussed above, can therefore cause uncertainty in the charged defect formation energies. However, our result that the formation energies for $\text{As}_i - \text{As}$ are at least 2 eV higher than the formation energies for As_{Ga} does indicate that equilibrium concentrations of $\text{As}_i - \text{As}$ should be significantly lower than equilibrium concentrations of As_{Ga} , as discussed below in Section 2.1(b).

In Figure 1 on the next page, we compare the results of formation energy calculations for $\text{As}_i - \text{As}$ in which both cell size and \mathbf{k} -space sampling methods have been varied. Most obvious in this figure is the wider variation in energies computed within the smaller supercell. Convergence with cell size is visibly slower when using the 1^3 MP mesh or the $\Gamma + \text{L}$ points. It is clear that the 217 atom cell with the 2^3 MP mesh is well converged. We see that the lower sampling schemes produce somewhat converged results in the 217 atom cell, as does the 2^3 MP mesh in the 65 atom cell. Similar to the results with defects in bulk Si,³⁷ we find that different sampling schemes can be used to produce either an attraction between defects (*i. e.* a lowering of energy in the smaller supercell), as in the 1^3 MP or $\Gamma + \text{L}$ cases, or a charge-state dependent repulsion or attraction between defects, as in the 2^3 MP case.

In the neutral charge state, the topmost filled electronic level is half filled, and corresponds to a localized state centered on the split interstitial. In Figure 2, the charge density associated with this defect state is shown in a plane parallel to an arsenic lattice plane, but slightly above this plane, so that it includes the two arsenic atoms of the split interstitial, which have relaxed slightly away from the ideal lattice site. This plot clearly shows that the defect state is localized in p-like orbitals which appear to be forming a π antibonding state, as is evident from

the node in the charge density midway between the two As atoms forming the split interstitial. This result is corroborated by an examination of the characterization of the defect state, which shows that in contrast to the very extended character of the bulk-like states, 20 % of the defect state is localized in the p_x and p_y orbitals of the two As atoms of the defect.

Figure 1. Defect formation energies for As_i -As computed in the As-rich limit. The Fermi energy varies from 0 (at the VBM) to the calculated conduction band edge. Comparisons are presented for different k -space sums and two supercell sizes. Dashed lines are used for cells containing 65 atoms and solid lines for 217 atom cells. Transition levels are marked with circles for the 2^3 MP mesh, squares for the 1^3 MP mesh, and triangles for the $\Gamma + L$ k -space sum.

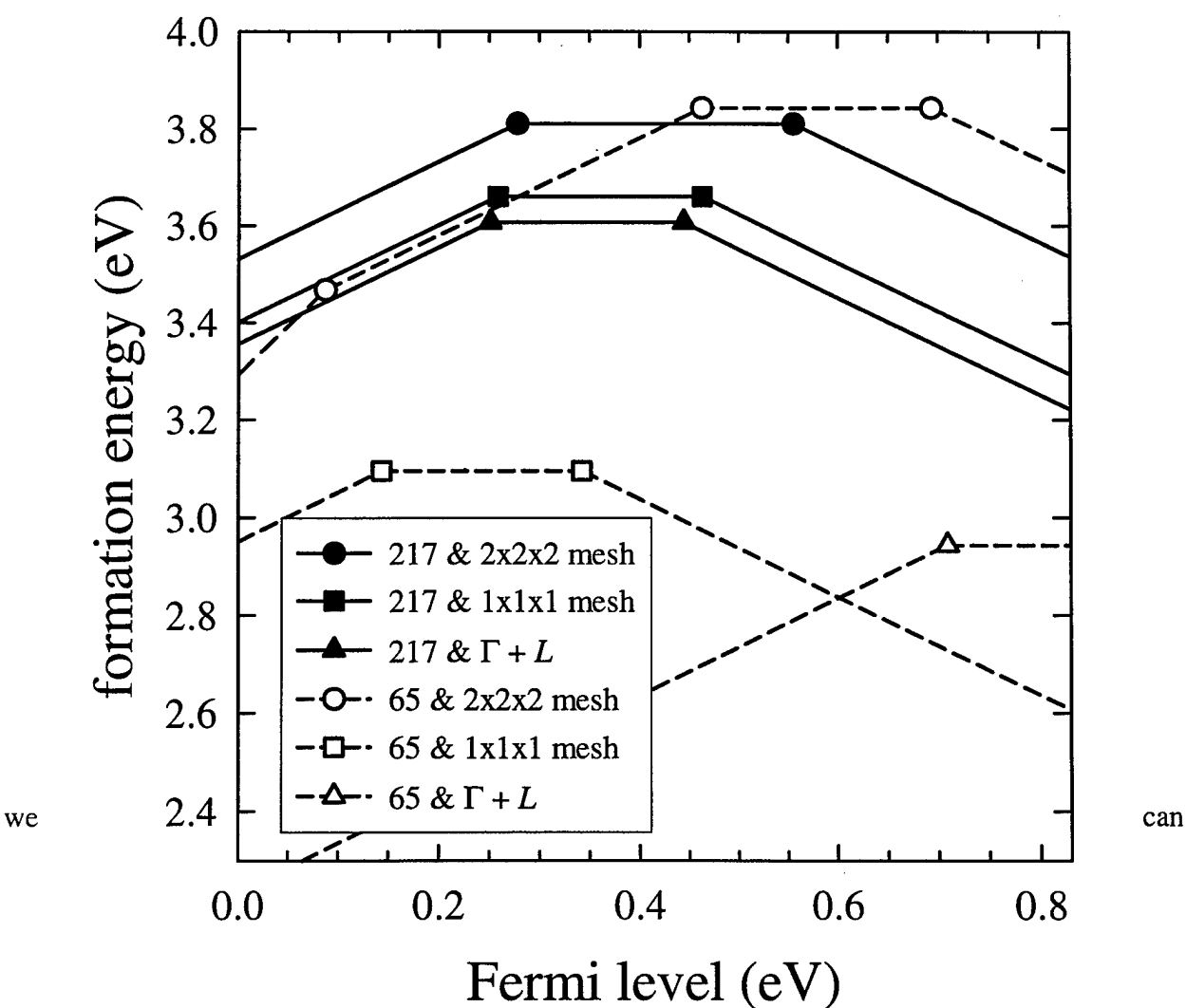
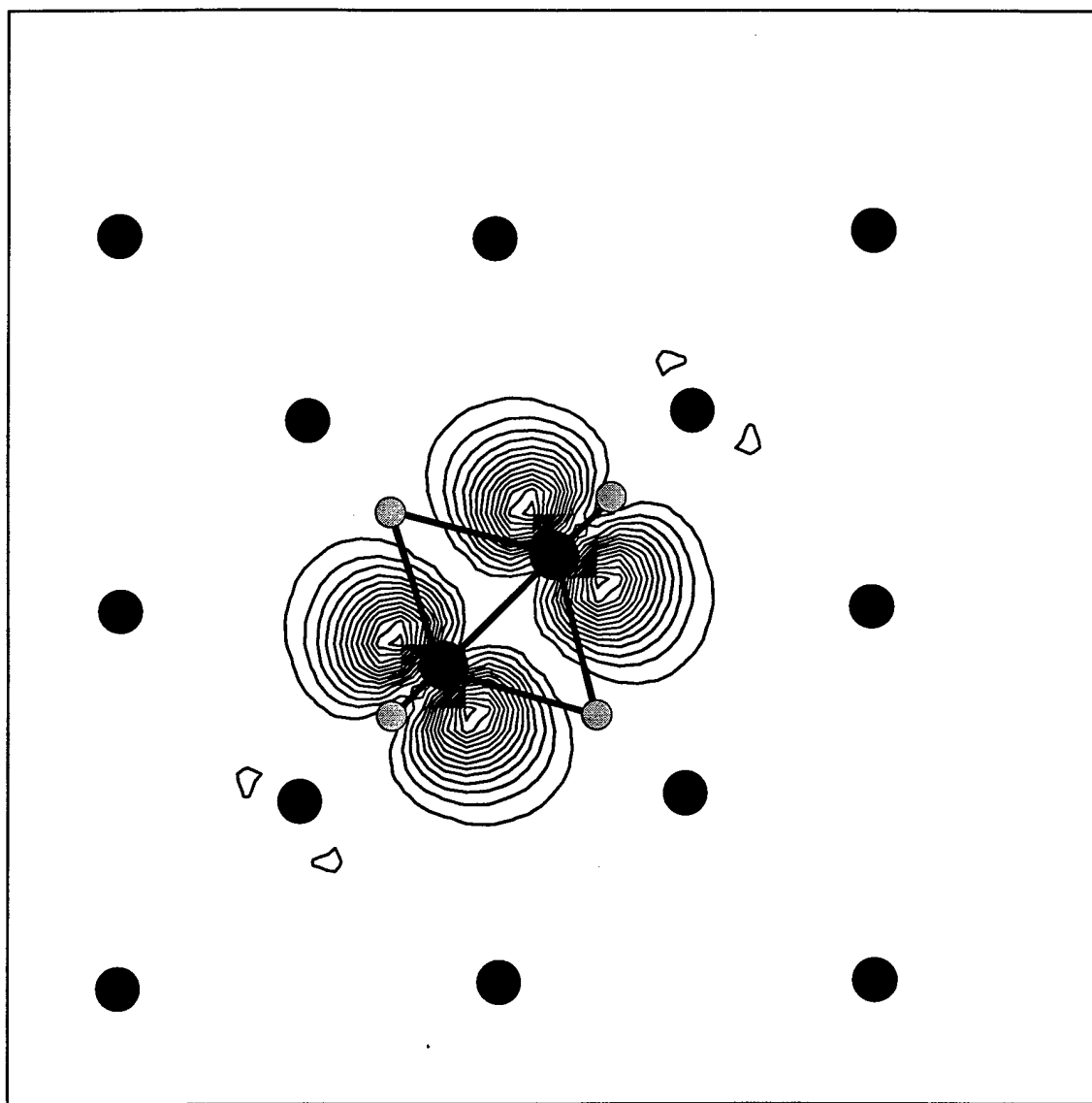


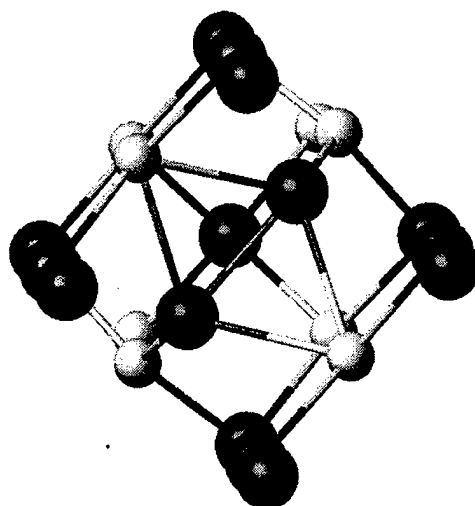
Figure 2. This contour plot shows levels of constant charge density for the localized defect state of the As_i -As, evaluated in the plane containing the two defect As atoms, which is 0.50 Angstroms above the As lattice site associated with the defect. The dark circles represent the positions of the As atoms, including the defect atoms and the As atoms of the original lattice plane. The gray circles show the locations of the neighboring Ga atoms projected onto the plane.



In smaller supercells, we found that the defect state interacts with its images and becomes less localized. One way to observe this is to examine the variation in energy of the defect state across \mathbf{k} -space, *i.e.* the dispersion of the state. We characterize this variation by computing the difference between the highest and lowest energy obtained from a \mathbf{k} -space survey. In the case of the 217 atom supercell, we find the maximum difference to be 0.1 eV, whereas we find the difference to be 0.5 eV in the 65 atom cell. This interaction of the defects in neighboring supercells contributes to the variations in the positions of the charge transition levels for different cell sizes and sampling schemes, and supports the conclusion that the larger 217 atom supercell should be used for accuracy in describing the charge transition levels and characterizing the deep defect states.

The detailed structure of the atomic positions for $\text{As}_i\text{-As}$ is also expected to be dependent on the cell size and \mathbf{k} -space sampling approach. However, we find that reasonable convergence is more easily reached for the atomic positions than for the electronic properties discussed above. In Figure 3, we show the structure of the neutral split interstitial viewed in a $[100]$ direction. The structure exhibits C_{2v} symmetry in all charge states, and returns to this symmetry when the atomic coordinates are perturbed from their equilibrium positions. The As-As and As-Ga distances found in the 65 atom supercell differ by less than 0.01 Angstroms from those found in

Figure 3. The neutral $\text{As}_i\text{-As}$ from the 217-atom supercell is shown (viewed from direction slightly displaced from the $[100]$ direction), with larger dark spheres representing the As atoms and the smaller light spheres representing the Ga atoms.



the 217 atom supercell. The distance between the two As atoms of the As_i -As defect is 2.39 Angstroms. (The GaAs bulk nearest neighbor distance in this calculation is 2.41 Angstroms.) Two Ga atoms are bonded to both As atoms of the defect, with an As-Ga separation of 2.60 Angstroms. The neighboring Ga atoms bonded to only one of the As of the split interstitial are separated from the As by 2.32 Angstroms. The distance between the two Ga that are bonded to both As defect atoms is 4.18 Angstroms, and the distance between the two atoms that are bonded to only one As defect atom is 4.37 Angstroms. The distance between either of the two Ga bonded to both As of the split interstitial and either of the two Ga bonded to only one atom of the defect is 4.32 Angstroms.

The two different supercell sizes produce slightly different results in the position of the center of mass of the two As atoms of the As_i -As. The center of mass of the pair of As atoms is shifted away from the original lattice site by 0.48 Angstroms in the [100] direction, toward the plane containing the two Ga atoms to which both As atoms are bonded, for the 217-atom supercell. This shift is 0.50 Angstroms in the smaller supercell. Since the nearest-neighbor distances are very similar in the two supercells, this difference is accomplished through variation of bond angles. The angle between the bonds from one of the As atoms to both of the Ga atoms that are bonded to both defect As atoms is 107.7° in the small supercell and 106.8° in the large supercell.

In the neutral charge state we find little correlation between the \mathbf{k} -space summation method and the defect bond lengths between the As atoms in the defect and between those As atoms and the four neighboring Ga atoms, in the 217 atom supercell. Each bond length differs by less than 0.1 % when the summation method is changed.

In the +1 charge state of the defect, we find a small relationship between the \mathbf{k} -space summation and the bond lengths. The As-As length obtained using $\Gamma + \text{L}$ sampling is about 1% larger than that obtained using the 2^3 MP mesh. The bond between either of the As atoms and one of the Ga atoms bonded to both As atoms is about 1 % shorter when using the $\Gamma + \text{L}$ summation method. The Ga bonded to only one As has a bond length about 0.5% shorter in the $\Gamma + \text{L}$ case than in the 2^3 MP mesh case.

There is a similar but even weaker effect (under 0.5%) in the defect bond lengths observed in the -1 state. The 1^3 MP mesh produces results between those of the other two k -space summation methods.

Focusing on results for the 217 atom cell with the 2^3 MP mesh, we observe that the distance between the atoms of the $\text{As}_i\text{-As}$ defect depends in a much more significant way on the charge state of the system. The As-As bond expands to 2.47 Angstroms (about 3.5 % compared to the neutral state bond length), when the system is allowed to relax in the -1 charge state. This is not surprising, since the antibonding defect state on the two As atoms is doubly occupied and can cause a stronger repulsive contribution to the interaction between these two atoms for the -1 charge state of the defect, while it is only singly occupied for the neutral state of the defect. The distance to the Ga bonded to both As atoms is 3 % smaller in the -1 state than in the neutral state, while the distance to the Ga bonded to only one of the As atoms is 1.5 % smaller in the -1 state.

When $\text{As}_i\text{-As}$ is in the +1 state, the As-As bond shrinks to 2.31 Angstroms, a contraction of about 3%. This is also not surprising, since in the +1 charge state, the antibonding defect state on the two As atoms of the defect is completely unoccupied. The Ga-As bond length for the Ga bonded to both As is 3.5 % longer and the Ga-As bond length for the Ga bonded to only one of the defect As atoms is 1.9 % longer in the +1 state than in the neutral state. We note that the two nearest neighbor Ga atoms bonded to both the As atoms move more dramatically when the charge state is changed. These Ga atoms in the -1 state are about 4 % closer to each other and in the +1 state are about 5.5 % farther apart than in the neutral state. The other two Ga atoms, each bonded to only one defect As atom, do not move in response to the change in charge state.

In performing these calculations, we fixed the lattice constant at the value determined through minimization of the energy of the bulk crystal in order to minimize artificial tensile or compressive strains. While the ideal calculation should include a full lattice constant determination with each change of defect configuration, for simplicity we did not perform this relaxation. This may be deemed a reasonable choice in light of evidence presented by Puska *et al.*³⁷ for *ab initio* supercell calculations in the LDA, using supercells of sizes comparable to ours, in which vacancies in bulk Si are found to alter the lattice constant by around 0.2 % while

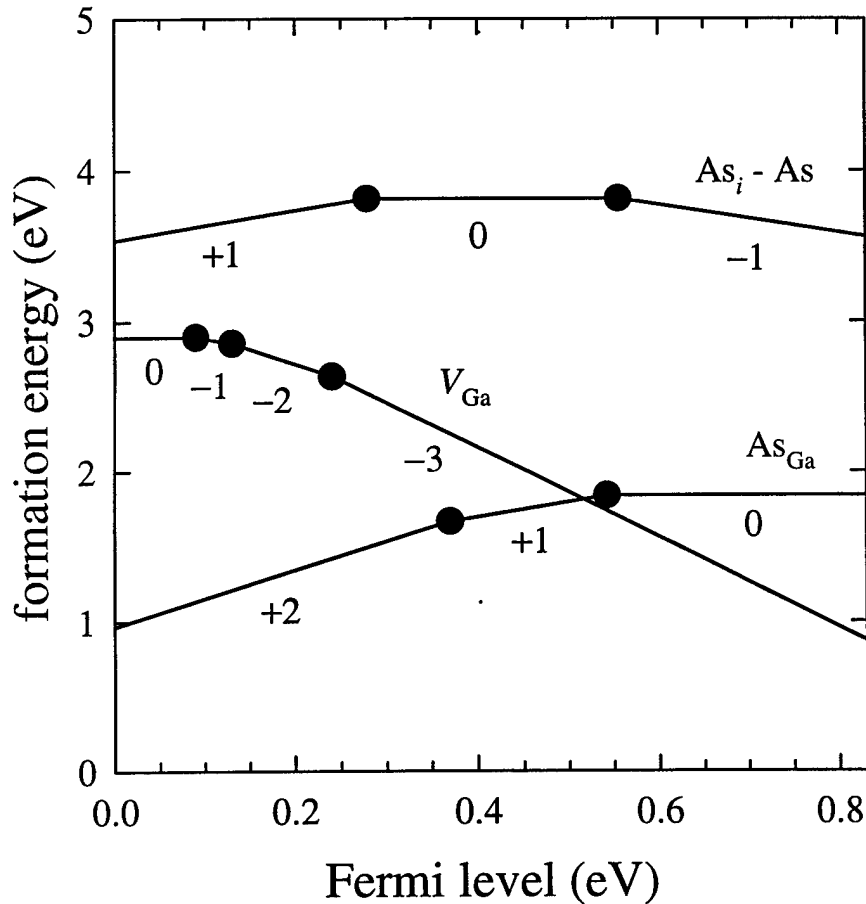
artificially introduced distortions in the lattice constant of up to 1 % are seen not to affect their reported results significantly.

In summary, we have shown that the calculated formation energies and transition levels of the arsenic split interstitial are strongly dependent on the size of a supercell, suggesting that large supercells are necessary when investigating these properties even though the arrangement of atoms in the structure may be converged in a smaller cell using the 2^3 MP mesh. Summation by k -space sampling also affects the results, but the difference between various sampling schemes becomes less significant for larger supercells. This result also reinforces the importance of the use of larger cells. To get a good description of charge state transition levels and a good characterization of the single deep defect level electronic state it is best to start with a 216 atom supercell.

2.1(b) Relative formation energies and equilibrium concentrations of native point defects containing excess arsenic in the As-rich limit

We now compare our well-converged results for the formation energies of the elementary excess-arsenic-containing point defects, As_{Ga} , V_{Ga} , and $\text{As}_i - \text{As}$ (the most favorable As_i configuration in semi-insulating or n-type GaAs), computed using the large supercell and the 2^3 MP mesh. These formation energies in the As-rich limit, corresponding to GaAs in equilibrium with bulk arsenic, are presented as a function of Fermi energy in Figure 4, on the next page. The formation energies for two specific choices of Fermi energy have also been listed in Table 1 in the previous section. As discussed above in Section 2.1(a), the formation energies of the charged defects depend on the position of the charge transition levels in the gap, so the uncertainty in the placement of these charge transition levels that is inherent in LDA calculations can cause uncertainty in the charged defect formation energies. However, we can see that the V_{Ga} and As_{Ga} defects possess significantly lower formation energies than $\text{As}_i - \text{As}$ for all Fermi energies, which should make them more common defects in the solid at thermal equilibrium than the $\text{As}_i - \text{As}$ defect.

Figure 4. Defect formation energies in the arsenic-rich limit as a function of Fermi energy, from the valence band edge (zero Fermi level) to the calculated conduction band edge.



To estimate equilibrium concentrations of As_{Ga} , V_{Ga} , and $\text{As}_i - \text{As}$ in As-rich GaAs, we begin with the usual expression for the equilibrium concentration of a defect

$$C = N \exp\{-\Delta E_f / (k_B T)\} \exp\{S_f / k_B\} \exp\{-P \Delta V_f / (k_B T)\},$$

where N is the number of sites per unit volume at which the defect can form, ΔE_f is the formation energy of the defect, k_B is the Boltzmann constant, and T is the temperature. The formation entropy of the defect is S_f , P is the pressure, and ΔV_f is the change in the crystal volume associated with the defect formation.

We note that the defect formation energy ΔE_f for charged defects, as given by the formula in the beginning of Section 2.1(a), has an explicit dependence on the Fermi energy, in addition to its dependence on the calculated energies for defect formation at zero Fermi energy. Therefore we must determine the Fermi energy self-consistently, in order to determine the native defect concentrations present in a particular sample. In order to do this, if any electrically active impurities or dopants are present in the material, the concentrations of the electrically active impurities or dopants in all charge states must also be taken into account. In order to determine the Fermi energy, one must solve self-consistently the charge balance equation, requiring that the free electron and hole concentrations (which also depend on the Fermi level) must cancel out any net charge resulting from the concentrations of all positively and negatively charged defects and impurities. Once the Fermi level is known, it may be used to determine the formation energies and the resulting equilibrium concentrations of all the defects present.

If the defect formation energy ΔE_f for the most energetically favorable charge state of $\text{As}_i\text{-As}$ in a particular sample is within $k_B T$ of the formation energy of the most favorable charge state of As_{Ga} , we may expect that the equilibrium concentrations of these two defects are comparable, assuming that the effects of the entropy of formation S_f and the change in the crystal volume ΔV_f associated with the defect formation can be neglected. We will now concentrate on the relative defect concentrations at 1500 K (near the melting point of GaAs), since defects with a higher formation energy such as $\text{As}_i\text{-As}$ have their greatest chance to attain equilibrium concentrations comparable to those of more energetically favorable defects at high temperature. We will estimate the effective corrections to the formation energy which occur at this temperature due to the entropy of formation and change in volume associated with the defects.

First, to estimate the effect of the change in volume, we let P be atmospheric pressure and overestimate ΔV_f be the volume per bulk atom in the cell, which gives an effective correction to the defect formation energy $P\Delta V_f$ of 9×10^{-5} eV. We may safely neglect this correction.

Previous calculations⁴⁸ on defects in Si found that the formation entropy S_f is dominated by vibrational contributions, and that the formation entropies are $6 k_B$ and $5 k_B$ for the self-interstitial and the vacancy, respectively. We note that the self-interstitial in silicon is a $\langle 110 \rangle$ split interstitial with the same basic structure as $\text{As}_i\text{-As}$ in GaAs. Therefore, in analogy to the

results for defects in silicon,⁴⁸ we may assume that it is unlikely for the split interstitial $\text{As}_i\text{-As}$ to have a very different formation entropy when compared to defects such as As_{Ga} , which only contain atoms occupying lattice sites. However, let us assume that this is the case. If we let $S_f = 10 k_B$ (an overestimate) for $\text{As}_i\text{-As}$, this gives rise to an effective reduction of the defect formation energy by $S_f T$, or 1.3 eV at 1500 K. Even if we apply no reduction to the As_{Ga} formation energy due to entropy, this still leaves the effective formation energy about 0.7 eV higher for $\text{As}_i\text{-As}$ than for As_{Ga} , producing equilibrium concentrations of $\text{As}_i\text{-As}$ which are about 0.4 % those of As_{Ga} at 1500 K.

These very liberal estimates for the effects of entropy in increasing the relative concentrations of $\text{As}_i\text{-As}$ rule out the likelihood that $\text{As}_i\text{-As}$ will attain a concentration approaching that of the antisites in thermal equilibrium.

2.1(c) Charge transition levels in the experimental gap

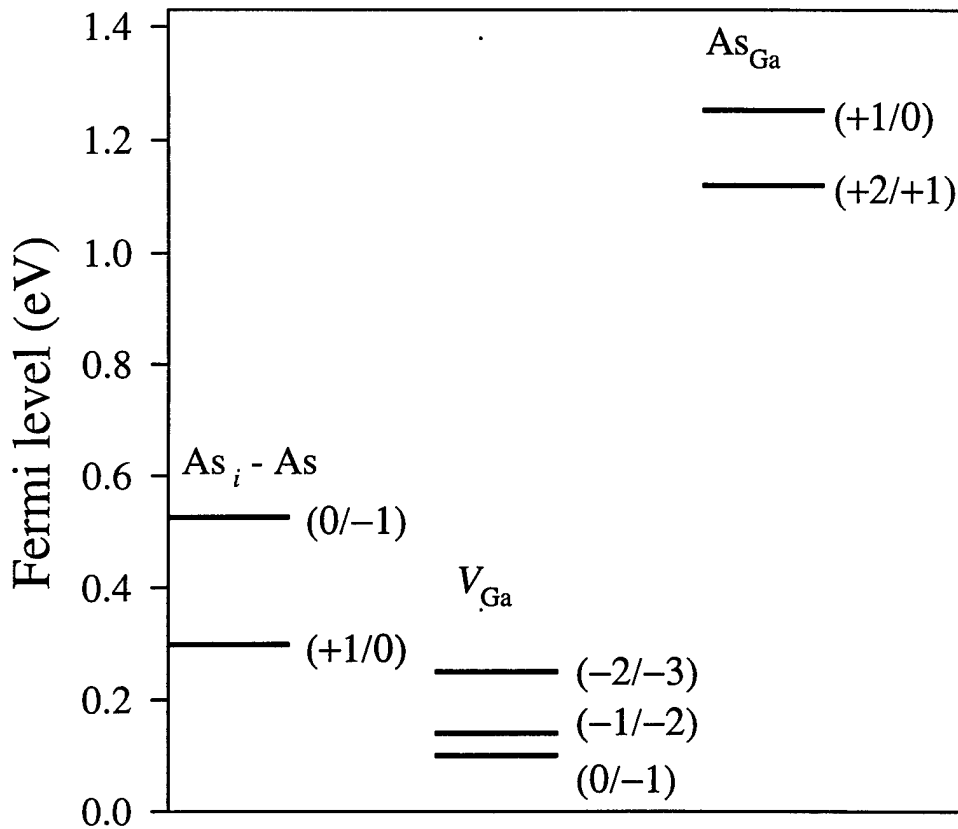
Although the placement of the calculated charge transition levels in the experimental gap has an uncertainty far exceeding 0.1 eV due to the shortcomings of the LDA in calculating the gap, as discussed in section 2.1(a), our as-calculated band gap and charge transition levels are reported here to 0.1 eV (or 0.01 eV, for the closely spaced V_{Ga} levels), for the convenience of the reader who prefers not to read them off the picture in Figure 4. For the As_{Ga} , the (+2/+1) transition level appears at 0.4 eV above the VBM and the (+1/0) level is at $E_{\text{VBM}} + 0.5$ eV. For the $\text{As}_i\text{-As}$, the (+1/0) transition is at $E_{\text{VBM}} + 0.3$ eV, and the (0/-1) transition is at $E_{\text{VBM}} + 0.5$ eV. The levels for the V_{Ga} defect are at 0.09 eV, 0.13 eV, and 0.2 eV above the VBM for the (0/-1), (-1/-2), and (-2/-3) transitions, respectively. The calculated zero-temperature band gap of 0.8 eV is underestimated by 0.7 V compared to the experimental zero-temperature gap of 1.5 eV.

As discussed previously in Section 2.1(a), the currently accepted approach for correcting the gap and the placement of the deep defect levels within the gap is to shift the conduction band derived states (including the deep defect states with primarily conduction band character) by the amount needed to correct the gap, while leaving the defect states with predominantly valence band character fixed relative to the valence band edge. Since the acceptor levels of the V_{Ga} are

derived from the dangling bonds on the arsenic neighbors of the vacancy, which require three extra electrons to fill them, they should have the predominantly valence band character of anion dangling bond states. In Section 2.1(a), the deep defect state of the $\text{As}_i\text{-As}$ was shown to have predominantly arsenic p-type character, similar to the character of the valence band edge states. However, the As_{Ga} double donor defect state derives from an antibonding state of predominantly conduction band character, which has been lowered in energy due to the replacement of the original anion-cation bonds of the ideal crystal by anion-anion bonds between the antisite and its nearest neighbors. This donor state is occupied by the two extra electrons contributed by the arsenic atom which has been substituted for a gallium atom, which cannot be accommodated in the bonding states of the valence band.

We conclude that the charge transition levels of the V_{Ga} and the $\text{As}_i\text{-As}$ should remain fixed relative to the valence band edge, while the charge transition levels of As_{Ga} , which possesses a conduction band character, should be shifted up together with the conduction band states. In Figure 5 on the following page, we show the charge transition states for these defects corrected by the above procedure, using the room temperature gap of 1.4 eV. The transition levels of As_{Ga} are shifted to 1.0 eV and 1.1 eV, in fortuitously good agreement with MCDA results in LT GaAs identified with this defect.²²

Figure 5. Charge transition levels for the excess-arsenic-containing point defects in GaAs, computed with a rigid shift applied to the conduction band and conduction band derived states to correct the LDA band gap underestimate and reproduce the room temperature gap of 1.4 eV.



2.1(d) Arsenic interstitial diffusion

Although we have found that equilibrium concentrations of arsenic interstitials cannot approach equilibrium concentrations of arsenic antisites in arsenic-rich, semi-insulating or n-type GaAs, there is experimental evidence that arsenic interstitials can play an important role in non-equilibrium processes, such as diffusion and compositional intermixing at interfaces, as discussed in Section 2.1.

Mr. Papoulias has investigated arsenic interstitial diffusion, following on from some preliminary work by Ms. Tischler. He has considered the role played by each of the three possible charge states of the split interstitial $\text{As}_i\text{-As}$ in the diffusion of this defect. Since he has focused on diffusion of the arsenic split interstitial in semi-insulating or n-type material, the interstitial is expected to start out in the -1 charge state. However, the interstitial can change to the neutral or $+1$ charge state at a cost given by the energy difference between the Fermi level ϵ_F and the transition energy for the transition to the desired charge state. This additional energy cost must be added to the migration barrier for diffusion in the new charge state to get a total effective energy barrier for changing charge followed by diffusion in the new charge state, which may be lower than the energy barrier for diffusion in the -1 charge state.

Since the $\text{As}_i\text{-As}$ sits on an arsenic site, it must hop to a second neighbor site in order to diffuse through the crystal. In order to fully understand $\text{As}_i\text{-As}$ diffusion, it has been necessary for Mr. Papoulias to investigate the lowest energy diffusion path and diffusion barrier for $\text{As}_i\text{-As}$ hops to a second neighbor along the bonding chain in the direction of the $\langle 110 \rangle$ interstitial axis, without and with a simultaneous reorientation of the interstitial axis, and hops to other second neighbor sites, also without and with a simultaneous reorientation of the interstitial axis.

A three step scheme has been employed to determine the height of the barrier faced by the As interstitial in one particular charge state, making one of these hops. First, the potential energy surface in the region of the path is investigated by stepping the moving As atom along, and holding a few critical distances fixed while relaxing the other atomic coordinates. Once the potential energy surface is understood sufficiently that good starting points for a transition state search can be identified, the ridge method⁴⁹⁻⁵⁰ is used to locate the transition state more precisely, and determine the energy barrier. The initial investigation and the initial transition state search are done with a 65-atom supercell and a 1^3 MP mesh, and then the transition state search is repeated with a 2^3 MP mesh to obtain a more accurate barrier, starting from the transition state configuration found with the 1^3 MP mesh. In agreement with our convergence results reported in Section 2.1(a), the atomic configuration of the transition state is already rather well converged with the 1^3 MP mesh, and does not change significantly when the \mathbf{k} -point mesh is changed. Finally, molecular dynamics at zero temperature is performed, starting at the transition state point

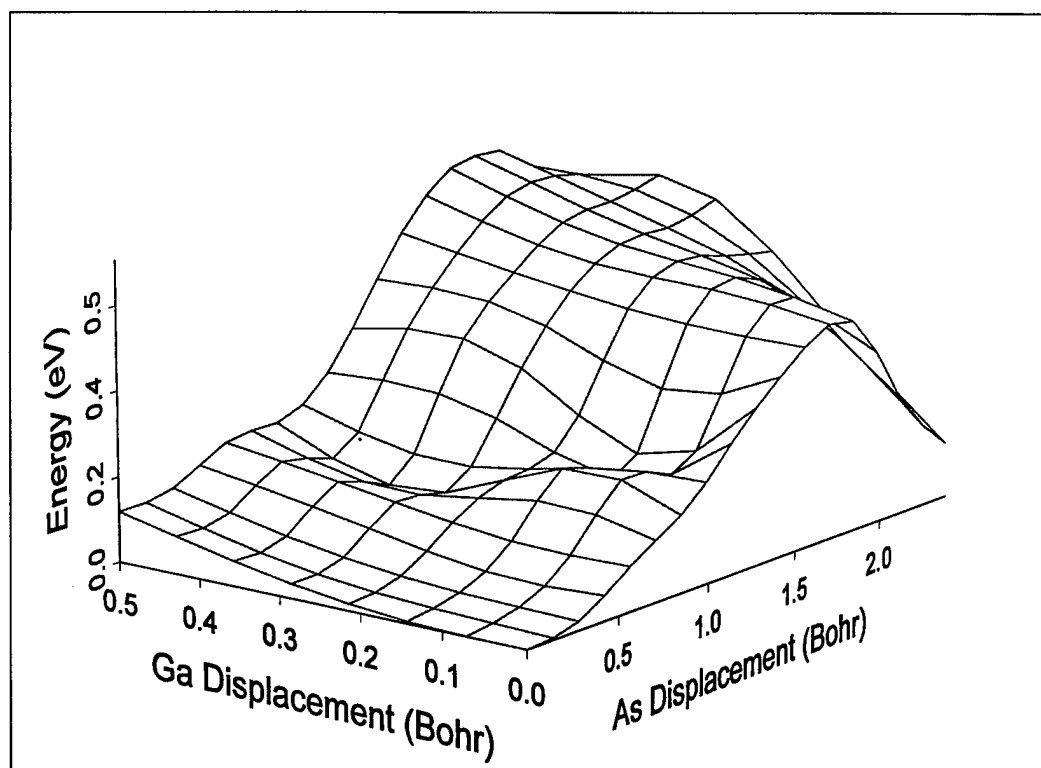
with a small bias to help the diffusing As to “roll” down either side of the potential hill, in order to obtain the entire lowest-energy path.

As an example of this method, Figure 6 on the following page shows the potential energy surface obtained for a neutral As_i -As hopping along the bonding chain in the direction of the interstitial axis, without a simultaneous change in direction of the interstitial axis. The barrier height estimated from this potential energy surface is about 0.5eV. After using the ridge method to locate the transition state more precisely, the barrier height was reduced to 0.4 eV. The transition state search calculation was then repeated with a $2 \times 2 \times 2$ \mathbf{k} -point mesh to produce the final, most accurate value for the barrier of 0.3eV.

The energy cost for the As_i -As to change from a -1 charge state to a neutral charge state, which will depend on the Fermi level, must be added to this barrier in order to obtain an effective barrier for the diffusion by this mechanism. However, for certain Fermi levels, this mechanism appears to be favored for this particular interstitial hop.

A full discussion of Mr. Papoulias's results for As_i -As diffusion, showing barriers that are reasonably consistent with the migration energy of 0.5 eV for arsenic interstitials deduced from annealing experiments on defects produced by electron irradiation,⁹ as well as migration energies subsequently ascribed to arsenic interstitial defects produced in GaAs by other means, will be available in his Ph.D. thesis.³⁹

Figure 6. Potential energy surface for the neutral arsenic interstitial diffusion hop which is discussed in the text. The arsenic displacement for the moving arsenic atom is measured from its initial position as one of the two atoms of the $\text{As}_i\text{-As}$, and the gallium displacement measures the displacement of the gallium neighbor atom which is bonded to the moving arsenic both before and after it hops over to become part of an $\text{As}_i\text{-As}$ on the second-neighbor arsenic site.



2.2 Arsenic Interstitial Pairs: Beginnings of an Interstitial Cluster

Although we have found that equilibrium concentrations of the lowest-energy arsenic split interstitials will be lower than equilibrium concentrations of arsenic antisites in arsenic-rich GaAs, as discussed in Section 2.1(b), there may be high non-equilibrium concentrations of arsenic interstitials as well as of other defects in GaAs, as a result of growth or processing. Hurle

has concluded from his extensive analysis¹⁰⁻¹² of experimental data that the deviation from stoichiometry in As-rich, melt-grown GaAs is due primarily to the creation of large numbers of electrically inactive arsenic interstitials during growth, while the less numerous arsenic antisites control the electrical behavior. Since isolated arsenic interstitials are electrically active, as discussed *e. g.* in Sections 2.1(a) and 2.1(c), this suggests that electrically inactive complexes of interstitials which do not involve antisites may sometimes be more numerous than any other defect. In early work⁵¹ supported by this grant and the parent AFOSR grant, F49620-96-1-0167, we have found that it is energetically favorable for two isolated arsenic interstitials to form a nearest-neighbor pair complex, consisting roughly of a split interstitial on an arsenic site and a split interstitial on an adjacent gallium site, and that this complex is electrically inactive (*i.e.* it will remain neutral for a Fermi level anywhere in the gap).

More recently, Mr. Papoulias has assisted in refining and extending these results by using the fully self-consistent, density-functional pseudopotential FHIMD code, with the 218-atom supercells and **k**-point sets required for accurate results, as discussed in section 2.1(a). One additional low-energy arsenic interstitial pair configuration was found, which has an energy lower by 0.1 eV than the energy of the nearest-neighbor interstitial pair.⁵² Although there is some uncertainty in the calculated charge transfer levels, due to the non-macroscopic size of the supercells as well as the well-known underestimation of the band gap for density-functional calculations, we find that both of these low-energy arsenic interstitial pair complexes will remain neutral for most Fermi energies in the gap.⁵² These two arsenic interstitial pair defects are shown in Figures 7 and 8 on the following page. For comparison, Figure 9 shows a higher energy neutral second-neighbor arsenic interstitial pair, consisting roughly of a two As_i-As interstitials on second neighbor arsenic sites, which has a formation energy 1.4 eV higher in energy than the lowest energy arsenic interstitial pair complex.

The formation energies for a neutral nearest-neighbor arsenic interstitial pair and for the lowest-energy arsenic interstitial pair are 5.7 eV and 5.6 eV, respectively, in the arsenic-rich limit (*i. e.* for GaAs in equilibrium with bulk arsenic).⁵² These formation energies may be compared with the formation energies from Table 1 in Section 2.1(a) for a neutral As_{Ga} and the neutral

Figure 7. The lowest energy arsenic interstitial pair, which involves three arsenic atoms sharing an arsenic site, forming an equilateral triangle.

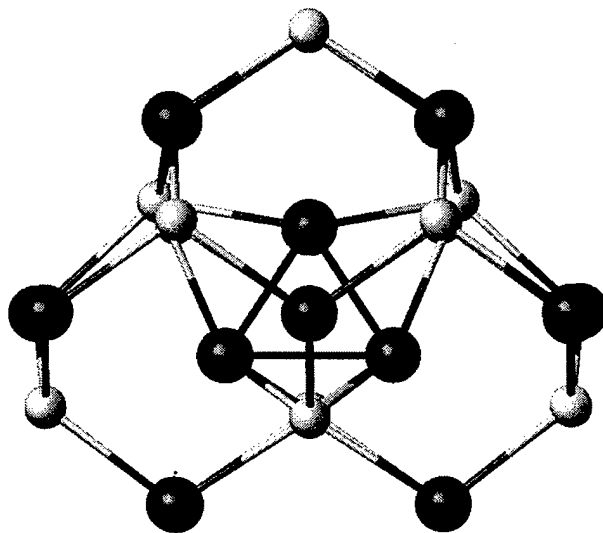


Figure 8. The nearest neighbor arsenic interstitial pair, which involves one additional arsenic atom sharing an arsenic site with the original arsenic atom, and one additional arsenic atom sharing the nearest-neighbor gallium site with the original gallium atom.

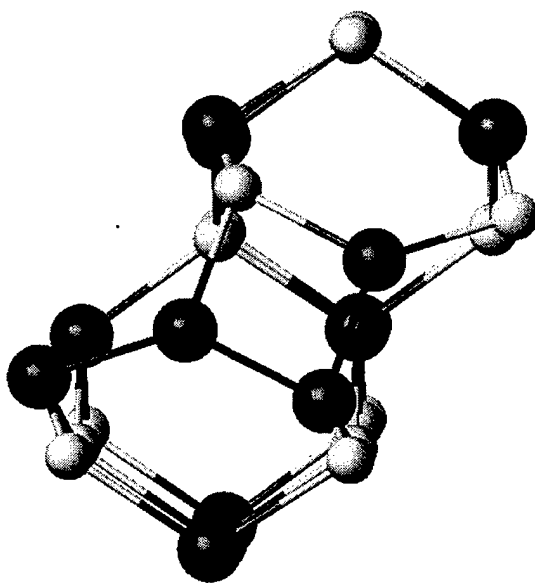
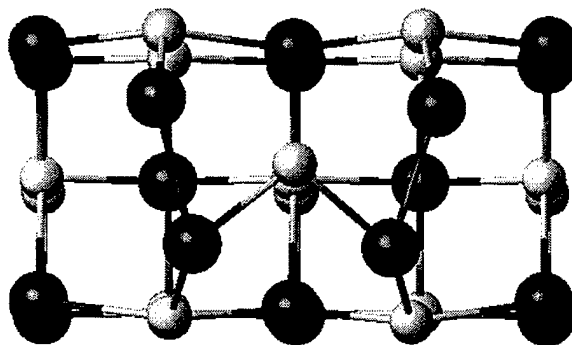


Figure 9. The neutral second neighbor arsenic interstitial pair, which involves two As_i -As defects on second nearest neighbor arsenic sites.



arsenic split interstitial As_i -As in the arsenic-rich limit, which are 1.8 eV and 3.8 eV, respectively.

Since the formation energy of the most energetically favorable arsenic interstitial pairs is higher than the formation energy for isolated arsenic interstitials by about 2 eV for a Fermi level anywhere in the gap, we conclude that equilibrium concentrations of arsenic interstitial pairs should be significantly lower than equilibrium concentrations of both isolated arsenic interstitials and arsenic antisites. However, if large, non-equilibrium concentrations of arsenic interstitials are present in GaAs as a result of growth and/or processing, we find that two isolated neutral interstitials can lower their energy by 2.0 or 1.9 eV by forming either of the two lowest energy interstitial pair complexes.⁵² With a binding energy of 2 eV, pair complexes should form rapidly in material with a large concentration of arsenic interstitials, perhaps serving as nuclei for the "interstitial clouds"¹⁵ which have been reported in some high-temperature-grown GaAs.

Recently, a combination of ion range calculations and molecular dynamics simulations using an empirical bond-order potential has been used to investigate the damage produced by MeV ion radiation of GaAs.⁵³ This study finds that extensive damage is produced by the ion bombardment, including many vacancies and interstitials in clusters and as isolated defects, and concludes that a clear majority of the isolated defects are interstitials. Ion bombardment of

silicon has also been found to induce interstitial clusters.⁵⁴⁻⁵⁶ We may consider these low energy arsenic interstitial pair complexes to represent the first stage of nucleation of an arsenic interstitial cluster in GaAs after radiation damage. They may also give us some ideas about the possible low-energy atomic structures of larger clusters.

2.3 Bond-order Potentials and Radiation Damage

The work in Reference 53 on identifying the atomic structures of the defects and larger defect clusters produced by radiation damage in GaAs may be considered as preliminary. For example, this work does not distinguish between Ga and As interstitials. The bond-order potential used in this work, which was fit by Karsten Albe, Kai Nordlund, Janne Nord, and Antti Kuronen, tries to fix some problems in earlier bond-order potentials proposed by others, and has been submitted to Phys. Rev. B, but this potential still has some remaining problems in describing both surfaces and defects. Its ability to describe the interstitials and interstitial clusters produced by irradiation is not yet well tested, since comparisons to DFT calculations for interstitials have only been done for tetrahedral interstitial configurations, not for the lowest energy split interstitial configurations. In order to describe the topological defect structures produced during irradiation, a bond-order potential should be fit to a complete set of state-of-the-art DFT calculations for the native defects in GaAs, and Karsten Albe is looking forward to using our results for this purpose.

3. Growth Processes and Incorporation of Excess As at Growth

The students whose research work was supported under this grant have also assisted with some of the calculations aimed at understanding the growth processes which control the incorporation of excess arsenic at the growing surface, which were begun under the AFOSR parent grant, F49620-96-1-0167. In particular, they have assisted with the simulated STM image generation for arsenic-decorated and gallium-decorated kinks on the GaAs growth surface.

3.1 Decorated and Undecorated Kinks: Structures, Formation Energies, and Contribution to Surface Stoichiometry

As has been described in the final report for the parent grant, we found that it would cost 0.7 eV for a single arsenic atom to adsorb in the trench on the ideal, kinkless $\beta 2(2 \times 4)$ surface, in the arsenic-rich limit corresponding to a surface in equilibrium with bulk arsenic, and 0.9 eV for an arsenic chemical potential corresponding to the calculated transition between the $\beta 2$ and the $c(4 \times 4)$ surface structures. Therefore, we do not expect appreciable numbers of single arsenic adatoms to be present on the ideal $\beta 2$ surface.

Near the transition between the $\beta 2$ and the $c(4 \times 4)$ surface structures, experiments often show the presence of the " $\gamma(2 \times 4)$ " surface, which resembles a disordered $\beta 2$ surface with some areas with wide trenches and many kinks in the mountain and trench rows. Based on our calculations of kink formation energies which were described in the final report for the parent grant, we have concluded that the additional amount of excess arsenic which is observed to be present in the " $\gamma(2 \times 4)$ " surface results from the adsorption of arsenic at the many kink sites which remain on the surface when the substrate temperature is too low to allow the kinks to anneal out. Some of the excess arsenic atoms in the trenches beside arsenic-decorated kink sites may become buried as growth proceeds, rather than being displaced by diffusing Ga adatoms, so these arsenic adatoms may act as precursors for As antisites.

Figure 10 on the next page shows the schematic structure of a line of bare (undecorated) kinks, seen from the top. We find that the energy cost to adsorb an arsenic atom at a bare kink to

form an arsenic-decorated kink is less than 0.1 eV for an arsenic chemical potential at the calculated transition between the $\beta 2$ and $c(4 \times 4)$ surfaces, much lower than the energy cost to adsorb an arsenic atom on the ideal $\beta 2$ surface. Figure 11 shows the schematic structure of a line of arsenic-decorated kinks, seen from the top. We find that the formation energy of a gallium-decorated kink, which resembles the arsenic-decorated kink but with the arsenic atom at the kink site replaced by a gallium atom, is only slightly higher than the formation energy of an arsenic-decorated kink for an arsenic chemical potential at the calculated transition between the $\beta 2$ and $c(4 \times 4)$ surfaces.

In order to allow experimentalists to differentiate between arsenic-decorated and gallium-decorated kinks in their surfaces, we have generated simulated STM images for these kinks, shown in Figures 12 and 13. Although the adatom in both cases prefers to remain within the angle of the kink, in the simulated filled-state STM picture for the arsenic-decorated kink we see the occupied dangling bond on the arsenic adatom sticking out toward the other side of the trench, while in the simulated filled-state STM picture for the gallium-decorated kink the gallium adatom has an empty dangling bond, so we see the filled bonding state which forms the bond from the gallium atom to the side wall, located in the angle of the kink.

Figure 10. Schematic picture of a line of undecorated kinks in the mountain and trench rows of the β_2 surface, seen from the top. The black atoms are arsenic, and the light gray atoms are gallium. The atoms in the top layers of the mountain are shown larger than the atoms in the top layer of the trench, since they are closer to the viewer.

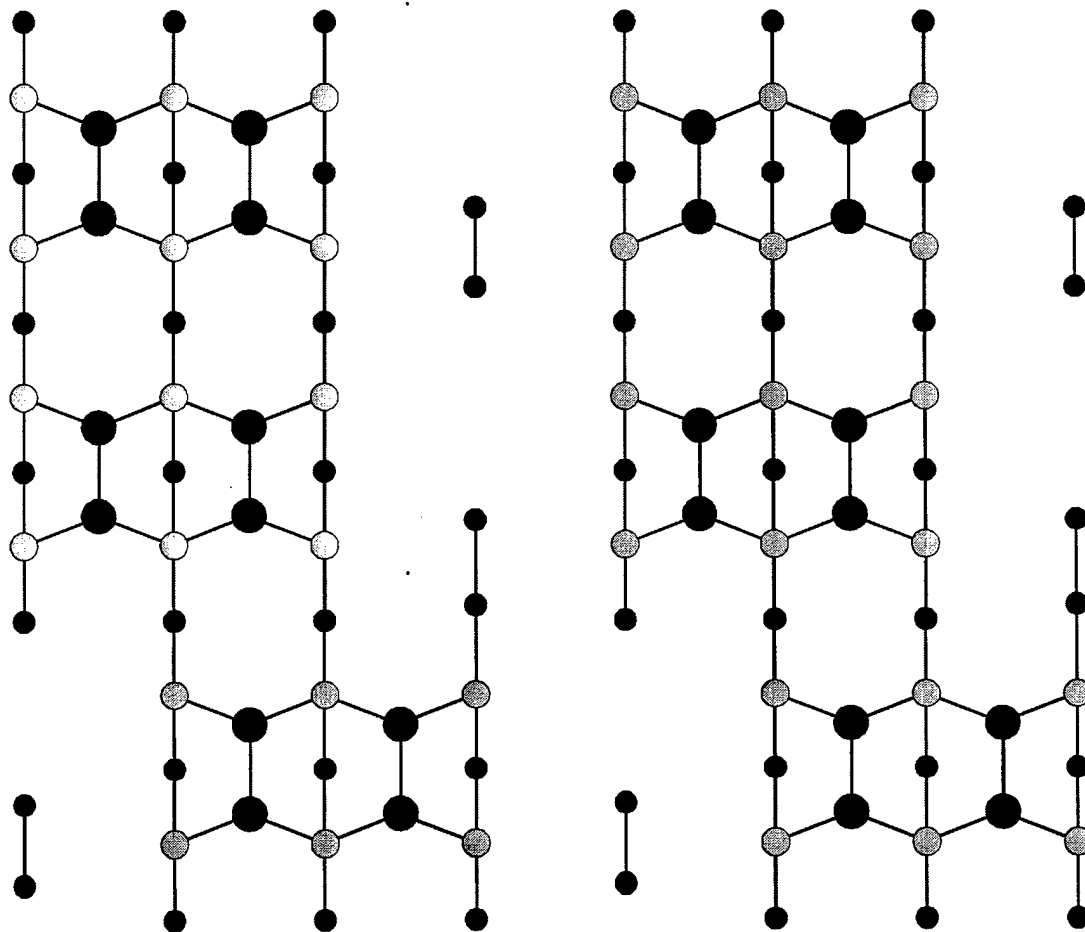


Figure 11. Schematic picture of a line of As-decorated kinks in the mountain and trench rows of the β_2 surface, seen from the top. The black atoms are arsenic, and the light gray atoms are gallium. The atoms in the top layers of the mountain are shown larger than the atoms in the top layer of the trench, since they are closer to the viewer.

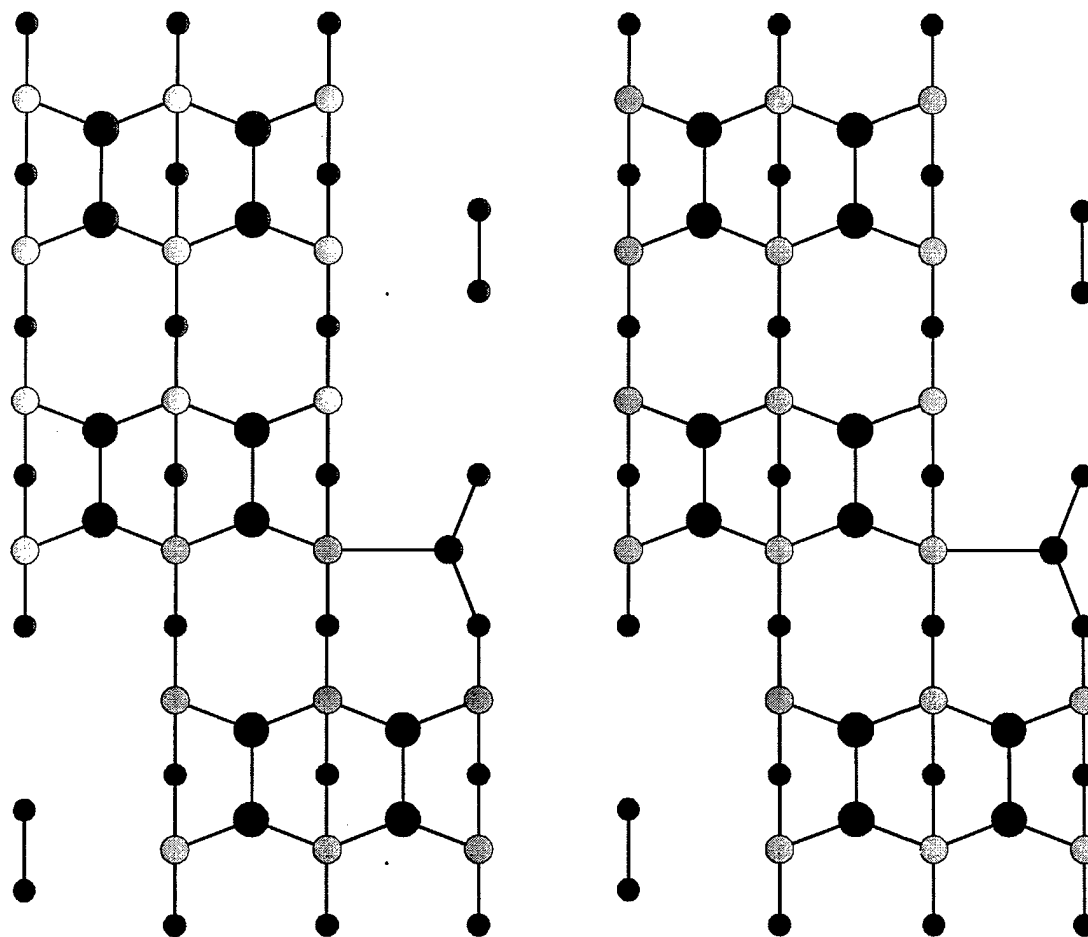


Figure 12. Simulated STM picture of an array of As-decorated kinks, seen from the top. There is one line of kinks at the top of the picture, one line in the middle, and one line at the bottom.

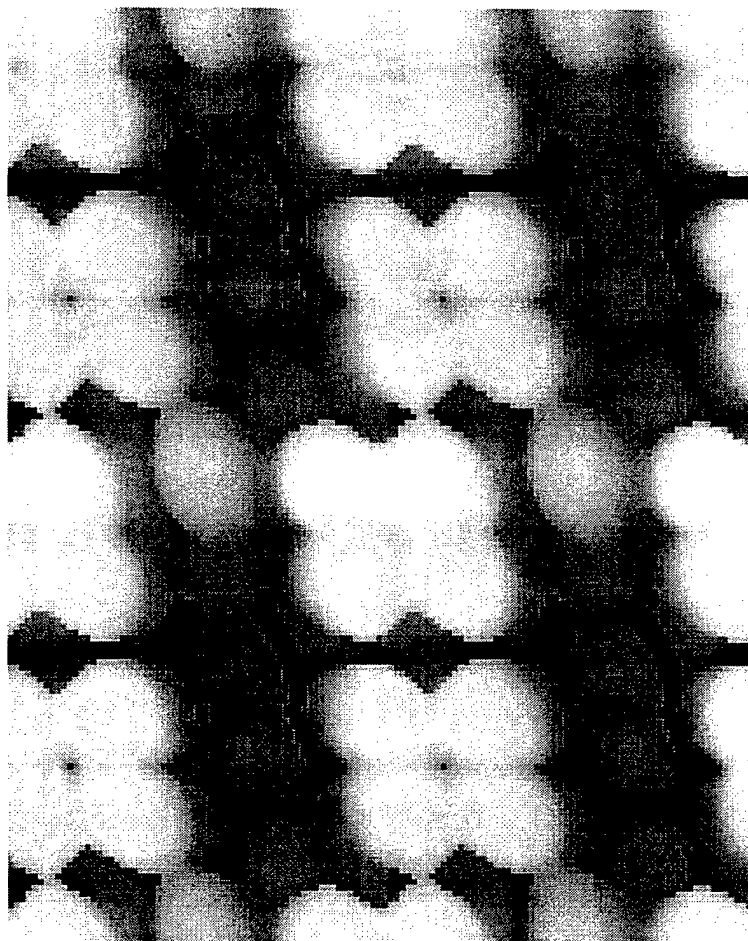
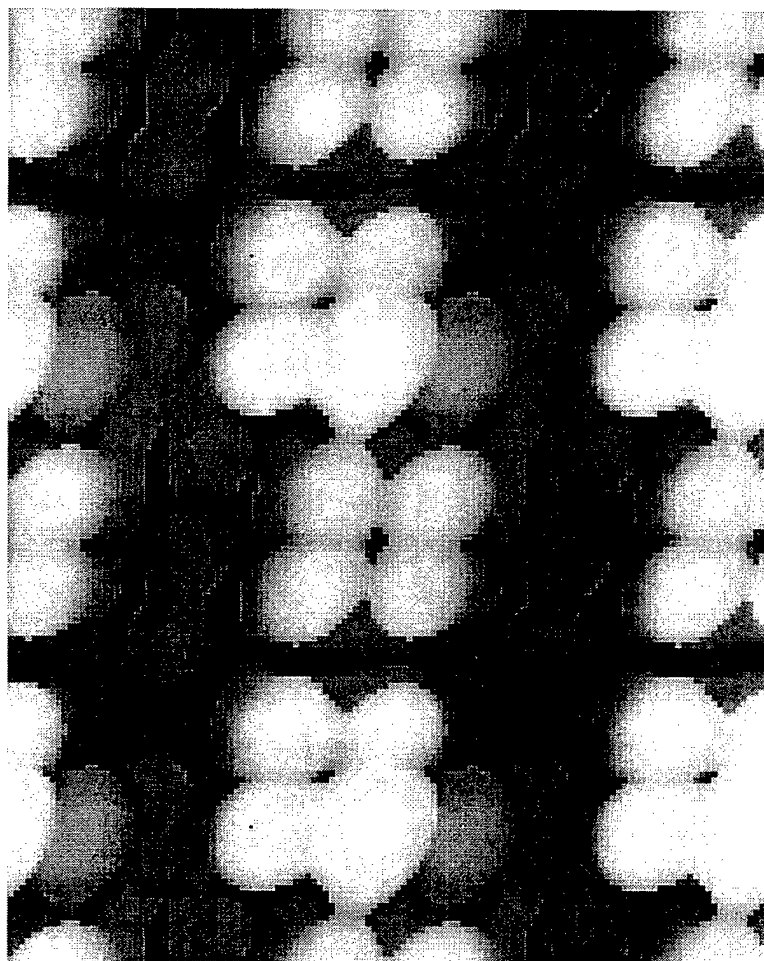


Figure 13. Simulated STM picture of an array of Ga-decorated kinks, seen from the top. There is one line of kinks at the top of the picture, one line in the middle, and one line at the bottom.



4. References

- ¹ J. Tersoff and D. R. Hamann, Phys. Rev. B **31**, 805 (1985).
- ² J. P. Perdew, K. Burke, and M. Ernzerhof, Phys. Rev. Lett. **77**, 3865 (1996).
- ³ O. F. Sankey and D. J. Niklewski, Phys. Rev. B **40**, 3979 (1989).
- ⁴ M. Bockstedte, A. Kley, J. Neugebauer, and M. Scheffler, Comput. Phys. Commun. **107**, 187 (1997).
- ⁵ D. R. Hamann, Phys. Rev. B **40**, 2980 (1989).
- ⁶ L. Kleinman and D. M. Bylander, Phys. Rev. Lett. **48**, 1425 (1982).
- ⁷ M. Fuchs and M. Scheffler, Comput. Phys. Commun. **119**, 67 (1999).
- ⁸ X. Gonze, R. Stumpf, and M. Scheffler, Phys. Rev. B **44**, 8503 (1991).
- ⁹ J. C. Bourgoin, H. J. von Bardeleben, and D. Stievenard, J. Appl. Phys. **64**, R65 (1988).
- ¹⁰ D. T. J. Hurle, J. Appl. Phys. **85**, 6957 (1999).
- ¹¹ D. T. J. Hurle, Materials Science Forum **196-201**, 179 (1995).
- ¹² D. T. J. Hurle, *Non-Stoichiometry ion Semiconductors* (Elsevier, New York, 1992), p. 47.
- ¹³ O. Oda, Semiconductor Science and Technology **7**, A215 (1992).
- ¹⁴ V. T. Bublik, Sov. Phys. Crystallog. **18**, 218 (1973).
- ¹⁵ L. Charniy and V. Bublik, J. Crystal Growth **135**, 302 (1994).
- ¹⁶ L. Charniy et al., J. Crystal Growth **118**, 163 (1992).
- ¹⁷ L. Charniy et al., J. Crystal Growth **116**, 369 (1992).
- ¹⁸ I. Fujimoto, Materials Science and Engineering **B14**, 426 (1992).
- ¹⁹ D. D. Nolte, J. Appl. Phys. **85**, 6259 (1999).
- ²⁰ K. M. Yu, M. Kaminska, and Z. Liliental-Weber, J. Appl. Phys. **72**, 2850 (1992).

- ²¹ M. Kaminska, Z. Liliental-Weber, E. R. Weber, T. George, J. B. Kortright, F. W. Smith, B-Y. Tsaur, and A. R. Calawa, *Appl. Phys. Lett.* **54**, 1881 (1989).
- ²² X. Liu, J. Nishio, E. R. Weber, Z. Liliental-Weber, and W. Walukiewicz, *Appl. Phys. Lett.* **67**, 79 (1995).
- ²³ R. M. Feenstra, J. m. Woodall, and G. D. Pettit, *Phys. Rev. Lett.* **71**, 1176 (1993).
- ²⁴ M. Luysberg, H. Sohn, A. Prasad, P. Specht, Z. Liliental-Weber, E. R. Weber, J. Gebauer, and R. Krause-Rehberg, *J. Appl. Phys.* **83**, 561 (1998).
- ²⁵ T. E. M. Staab, R. M. Nieminen, J. Gebauer, R. Krause-Rehberg, M. Luysberg, M. Haugk, and T. Frauenheim, *Phys. Rev. Lett.* **87**, 045504 (2001).
- ²⁶ M. Schultz, U. Egger, R. Scholz, O. Breitenstein, U Gösele, *J. Appl. Phys.* **83**, 5295 (1998).
- ²⁷ V. V. Chaldyshev, N. A. Bert, Y. G. Musikhin, A. A. Suvorova, V. V. Preobrazhenskii, M. A. Putyato, B. R. Semyagin, P. Werner, and U Gösele, *Appl. Phys. Lett.* **79**, 1294 (2001).
- ²⁸ G. A. Baraff and M. Schlüter, *Phys. Rev. Lett.* **55**, 1327 (1985).
- ²⁹ R. W. Jansen and O. F. Sankey, *Phys. Rev. B* **39**, 3192 (1989).
- ³⁰ S. B. Zhang and J. E. Northrup, *Phys. Rev. Lett.* **67**, 2339 (1991).
- ³¹ D. J. Chadi, *Phys. Rev. B* **46**, 9400 (1992).
- ³² J. I. Landman, C. G. Morgan, J. T. Schick, P. Papoulias, and A. Kumar, *Phys. Rev. B* **55**, 15581 (1997).
- ³³ M.-H. Tsai, O. F. Sankey, and J. D. Dow, *Phys. Rev. B* **46**, 10464 (1992).
- ³⁴ D. J. Chadi and M. L. Cohen, *Phys. Rev. B* **8**, 5747 (1973).
- ³⁵ S. Pöykkö, M. J. Puska, M. Alatalo, and R. M. Nieminen, *Phys. Rev. B* **54**, 15513 (1996).
- ³⁶ G. Makov, R. Shah, and M. C. Payne, *Phys. Rev. B* **53**, 7909 (1996).
- ³⁷ M. J. Puska, S. Pöykkö, M. Pesola, and R. M. Nieminen, *Phys. Rev. B* **58**, 1318 (1998).
- ³⁸ J. T. Schick, C. G. Morgan, and P. Papoulias, "First-principles Study of As Interstitials in GaAs: Convergence, Relaxation, and Formation Energy", submitted to *Physical Review B*.

- ³⁹ P. Papoulias, Ph.D. thesis, in preparation.
- ⁴⁰ P. Hohenberg and W. Kohn, Phys. Rev. **136**, 13187909 (1998).
- ⁴¹ D. M. Ceperley and G. J. Alder, Phys. Rev. Lett. **58**, B864 (1964).
- ⁴² J. Perdew and A. Zunger, Phys. Rev. B **23**, 5048 (1981).
- ⁴³ L. Kleinman, Phys. B **24**, 7412 (1981).
- ⁴⁴ A. F. Kohan, G. Ceder, D. Morgan, and C. G. Van de Walle, Phys. Rev. B **61**, 15019 (2000).
- ⁴⁵ K. A. Johnson and N. W. Ashcroft, Phys. Rev. B **58**, 15548 (1998).
- ⁴⁶ H. J. Monkhorst and J. D. Pack, Phys. Rev. B **13**, 5188 (1976).
- ⁴⁷ D. J. Chadi, P. H. Citrin, C. H. Park, D. L. Adler, M. A. Marcus, and H.-J. Gossman, Phys. Rev. Lett. **79**, 4834 (1997).
- ⁴⁸ P. E. Blöchl, E. Smargiassi, R. Car, D. B. Laks, W. Andreoni, and S. T. Pantelides, Phys. Rev. Lett. **70**, 2435 (1993).
- ⁴⁹ I. V. Ionova and E. A. Carter, J. Chem. Phys. **98**, 6377 (1993).
- ⁵⁰ I. V. Ionova and E. A. Carter, J. Chem. Phys. **103**, 5437 (1995).
- ⁵¹ P. Papoulias, C. G. Morgan, J. T. Schick, J. I. Landman, and N. Rahhal, Materials Science Forum **258-263**, 923 (1997).
- ⁵² J. T. Schick, C. G. Morgan, and P. Papoulias, "Nearest-Neighbor As Interstitial Pairs in GaAs: a First Stage for As Clusters?", submitted to Phys. Rev. B.
- ⁵³ K. Nordlund, J. Peltola, J. Nord, J. Keinonen, and R. S. Averback, J. Appl. Phys. **90**, 1710 (2001).
- ⁵⁴ N. E. B. Cowern, G. Mannino, P. A. Stolk, F. Roozeboom, H. G. A. Huizing, J. G. M. van Berkum, F. Cristiano, A. Claverie, and M. Jaraiz, Phys. Rev. Lett. **82**, 4460 (1999).
- ⁵⁵ L. A. Marques, L. Pelaz, J. Hernandez, J. Barbolla, and G.H. Gilmer, Phys. Rev. B **64**, 045214 (2001).
- ⁵⁶ S. Libertino, S. Coffa, and J. L. Benton, Phys. Rev. B **63**, 195206 (2001).

5. Students Supported under this Grant

Graduate Students

Joseph I. Landman, supported by other funds, but used resources maintained under this grant in the preparation of his Ph.D. thesis in 1997.

Panagiotis Papoulias, supported in part by this grant, and even during the periods when he was supported by other funds, he used resources maintained under this grant in his research and the initial stages of writing his Ph.D. thesis, 1997-2001.

Sean McGee, supported by this grant, 2000-2001.

Undergraduate Students

Andrea Bursott, Sept.-Dec. 1998

Lisa Horn, Sept.-Dec. 1998

Christopher Bush, Sept. 1998 - Oct. 1999

6. Publications/Presentations/Degrees Granted

Publications for which the major work was done by students whose research was supported by this AASERT grant:

(See also the report for the AFOSR parent grant, F49620-96-1-0167, for additional publications by the other members of the research team, with smaller contributions by AASERT-supported students.)

"Arsenic Interstitials and Interstitial Complexes in Low-Temperature-Grown GaAs," J.I. Landman, C.G. Morgan, J. T. Schick, P. Papoulias, and A. Kumar, Physical Review B **55**, 15581-15586 (1997).

"Arsenic Interstitial Pairs in GaAs", P. Papoulias, C. G. Morgan, J. T. Schick, J. I. Landman, and N. Rahhal, Materials Science Forum **258-263**, 923-928 (1997).

"First-principles Study of As Interstitials in GaAs: Convergence, Relaxation, and Formation Energy", J. T. Schick, C. G. Morgan, and P. Papoulias, submitted to Physical Review B.

"Nearest-Neighbor As Interstitial Pairs in GaAs: a First Stage for As Clusters?", J. T. Schick, C. G. Morgan, and P. Papoulias, submitted to Physical Review B.

"Substitutional Be and its Interactions with As Antisites in GaAs", P. Papoulias and C. G. Morgan, in preparation.

"As Interstitial Diffusion in GaAs", P. Papoulias, C. G. Morgan, and J. T. Schick, in preparation.

Presentations with major contributions by students supported by this AASERT grant:

(See also report for the AFOSR parent grant, F49620-96-1-0167, for additional contributed and invited presentations by the other members of the research team.)

"Arsenic Interstitial Pairs in GaAs", P. Papoulias, C. G. Morgan, J. T. Schick, J. I. Landman, and N. Rahhal, 19th International Conference on Defects in Semiconductors, Aveiro, Portugal, July 21, 1997.

"Theory of Defect Structures in LT GaAs", C. G. Morgan, P. Papoulias, J. I. Landman, J. T. Schick, A. Tischler, and N. Rahhal, AFOSR Contract Review, UC Santa Barbara, Aug. 19, 1997.

“Arsenic Dimer Dynamics”, C. G. Morgan, P. Papoulias, P. Kratzer, and M. Scheffler, WSU Physics Colloquium, Dec. 3, 1998.

“First-Principles Studies of Growth Processes and Defects in LT GaAs”, C. G. Morgan, P. Papoulias, A. Tischler, and J. T. Schick, AFOSR Contract Review, Kettering OH, Sept. 28, 1999.

“Augmented Student Participation in Theoretical Investigation of Point Defects and Defect Complexes in Low-Temperature-Grown GaAs”, C. Morgan, P. Papoulias, and J. Schick, Supercomputing 2000, November 2000, Dallas, TX.

“Dynamic Processes, Defects, and Surfaces in Semiconductors”, C. G. Morgan, P. Papoulias, P. Kratzer, and M. Scheffler, Wayne State University, Dec. 12, 2000.

Degrees earned by students who have worked on this AASERT-funded research project

Joseph I. Landman, Ph. D., “A Molecular Dynamics Investigation of Low Temperature Gallium Arsenide”, thesis defense: July 18, 1997.

Panagiotis Papoulias, Ph.D., “Arsenic Interstitials and Interstitial-Containing Complexes in GaAs”, thesis in preparation.

In addition, the following student was an American citizen at the time her degree was awarded, but she did research work supported by the associated AFOSR parent grant, “Theoretical Investigation of Point Defects and Defect Complexes in Low-Temperature-Grown GaAs” (F49620-96-1-0167) before becoming a citizen, since she could not yet be supported under this AASERT grant:

Ana Tischler, M.A., “Diffusion in GaAs and GaAs-based Materials”, presentation/defense: April 14, 2000.